SVN Stroke & Vascular Neurology

miR-19-3p/GRSF1/COX1 axis attenuates early brain injury via maintaining mitochondrial function after subarachnoid haemorrhage

Ge Gao, Xiaoyu Sun, Jiajia Xu, Jian Yu, Yang Wang

To cite: Gao G, Sun X, Xu J, *et al*. *miR-19-3p*/GRSF1/COX1 axis attenuates early brain injury via maintaining mitochondrial function after subarachnoid haemorrhage. *Stroke & Vascular Neurology* 2024;**0**. doi:10.1136/svn-2024-003099

► Additional supplemental material is published online only. To view, please visit the journal online (https://doi.org/10.1136/svn-2024-003099).

GG, XS and JX contributed equally.

Received 6 January 2024
Accepted 30 July 2024

Department of Neurosurgery, The First Affiliated Hospital of USTC, Division of Life Sciences and Medicine, University of Science and Technology of China, Hefei, Anhui, China

Correspondence to
Dr Yang Wang; ahwy_neurosurgery@fsyy.ustc.edu.cn

Dr Jian Yu; yujianqi024@163.com

ABSTRACT

Background Guanine-rich RNA sequence binding factor 1 (GRSF1) is an RNA-binding protein, which is eventually localised to mitochondria and promotes the translation of cytochrome C oxidase 1 (COX1) mRNA. However, the role of the *miR-19-3*p/GRSF1/COX1 axis has not been investigated in an experimental subarachnoid haemorrhage (SAH) model. Thus, we investigated the role of the *miR-19-3*p/GRSF1/COX1 axis in a SAH-induced early brain injury (EBI) course.

Methods Primary neurons were treated with oxyhaemoglobin (OxyHb) to simulate in vitro SAH. The rat SAH model was established by injecting autologous arterial blood into the optic chiasma cisterna. The GRSF1 level was downregulated or upregulated by treating the rats and neurons with lentivirus-*GRSF1* shRNA (Lenti-*GRSF1* shRNA) or lentivirus-*GRSF1* (Lenti-*GRSF1*).

Results The *miR-19-3*p level was upregulated and the protein levels of GRSF1 and COX1 were both downregulated in SAH brain tissue. *GRSF1* silence decreased and *GRSF1* overexpression increased the protein levels of *GRSF1* and COX1 in primary neurons and brain tissue, respectively. Lenti-*GRSF1* shRNA aggravated, but Lenti-*GRSF1* alleviated, the indicators of neuronal injury and neurological impairment in both in vitro and in vivo SAH conditions. In addition, *miR-19-3*p mimic reduced the protein levels of GRSF1 and COX1 in cultured neurons while *miR-19-3*p inhibitor increased them. More importantly, Lenti-*GRSF1* significantly relieved mitochondrial damage of neurons exposed to OxyHb or induced by SAH and was beneficial to maintaining mitochondrial integrity. Lenti-*GRSF1* shRNA treatment, conversely, aggravated mitochondrial damage in neurons.

Conclusion The *miR-19-3*p/GRSF1/COX1 axis may serve as an underlying target for inhibiting SAH-induced EBI by maintaining mitochondrial integrity.

WHAT IS ALREADY KNOWN ON THIS TOPIC

⇒ Subarachnoid haemorrhage (SAH) is a common cerebrovascular emergency, often accompanied by serious complications. It has been reported that the mitochondrial dysfunction of injured neurons after SAH is the key factor leading to early brain injury. The abnormal mitochondrial function leads to the dysfunction of axons and even the whole neuron. As an important mechanism for the quality control of neuronal mitochondria, the mitochondrial respiratory chain function of neurons has become a topic of research interest in the neuroprotection field after SAH.

WHAT THIS STUDY ADDS

⇒ Our research confirmed that the *miR-19-3p*/GRSF1/COX1 signal axis is involved in the brain injury process induced by SAH and that the activation of this signal axis significantly mitigated post-SAH-induced mitochondrial dysfunction.

HOW THIS STUDY MIGHT AFFECT RESEARCH, PRACTICE OR POLICY

⇒ Our research clarifies the role of the *miR-19-3p*/GRSF1/COX1 axis and its mechanism under brain injury following SAH and provides new ideas and insights for treating patients with SAH.

INTRODUCTION

Spontaneous subarachnoid haemorrhage (SAH) is a common and critical neurological disease caused by the sudden rupture of an intracranial aneurysm resulting in rapid blood entry into the subarachnoid space, accounting for approximately 5%–7% of stroke cases.[1 2] Recent research suggests that early brain injury (EBI) following SAH may be the most common cause of death and disability in patients with SAH.[3 4] Therefore, overcoming EBI is the key to reducing mortality in this population.[5] Consequently, the investigation into the pathophysiological changes that occur after SAH and its pathogenesis represent urgent problems for neurotranslational medicine research and clinical work to identify effective key therapeutic targets.

Energy deprivation and dysfunction of nerve cells have crucial roles in the process of EBI.[6] Intracellular transport is crucial for the distribution and location of proteins and RNA in neurons and for the long-range information transmission of neurons.[7 8] Axons act as high-speed superhighways and control the body by continuously transmitting information.[9] 'Energy factory' mitochondria provide

energy for information exchange in axons.[10] Normal mitochondrial function is the energy security of nerve function, whereas abnormal mitochondrial function leads to dysfunction of axons and even the whole neuron.[11] After SAH, it has been reported that neuronal mitochondria are damaged and functional abnormality appears.[12]

The mitochondrial respiratory chain is mainly composed of various respiratory chain-related enzymes and defects of the respiratory chain enzyme complex are important causes of mitochondrial-related diseases.[13 14] Cytochrome C oxidase (COX) is one of the key terminal enzymes of the mitochondrial respiratory chain, which functions in the inner mitochondrial membrane by transferring electrons to O_2 to form H_2O and releasing protons into the mitochondrial membrane space. The COX complex contains multiple metal cofactors and subunits and is a macromolecular protein.[15 16] The COX1, COX2 and COX3 subunits of mammals are encoded by DNA located within mitochondria, which is highly conserved, and form certain catalytic reaction centres.[17] However, after SAH, the trend of COX1 protein levels and the regulatory factors in neuron mitochondria remains unclear.

As a semiautonomous organelle, mitochondria possess their own DNA (mitochondrial DNA), but the mitochondrial genetic system largely depends on the nuclear genetic system.[18] Professor Jean-Claude Martinou from Geneva University and his team have identified small compartments containing hundreds of different proteins in the mitochondrial centre where the mitochondria's RNA molecules gather and mature.[19 20] These chambers, which contain all of the enzymes needed for RNA maturation, have been named mitochondrial RNA granules.[21] It has been highlighted that the abnormalities of mitochondrial RNA particles may lead to many pathological processes related to mitochondria.[22] This is because the proteins in the mitochondrial RNA particles are synthesised under the guidance of the cell's nuclear DNA. It has been reported that Guanine-rich RNA sequence binding factor 1 (GRSF1) acts as an important RNA-binding protein to promote COX1 mRNA translation, which is transcribed by nuclear DNA and translated by cytoplasmic ribosomes, before eventually migrating to mitochondria.[23] Currently, the research on GRSF1 has mainly focused on the investigation of tumours. A recent study has also indicated that GRSF1 attenuates neuron ferroptosis in spinal cord injury and promotes functional recovery,[24] but, for the most part, it did not address SAH.

Previous studies have reported that approximately 30% of the human gene transcriptome is the direct target of microRNAs (miRNAs), and miRNAs regulate most human genes.[25] It is well known that gene regulation occurs faster and more accurately in the post-transcriptional stage than in the transcriptional stage. Hence, it may be more important in the regulation of the protein level during the acute stage of a stroke.[26] Through the TargetScanHuman (http://www.targetscan.org/), we predicted that *miR-19-3*p can target the *GRSF1* mRNA 3' untranslated regions (UTRs). *MiR-19-3*p is conserved in humans, rats and mice (online supplemental figure S1A), which was further verified by the double luciferase method. This result suggests that the transcription of GRSF1 may be regulated by *miR-19-3*p (online supplemental figure S1B). These reliable data suggest that the *miR-19-3*p/GRSF1/COX1 axis may provide novel therapeutic options for regulating SAH-induced EBI by maintaining mitochondrial respiratory chain integrity. However, these assumptions remain obscure and need to be further confirmed. In this experiment, we will explore the roles of the *miR-19-3*p/GRSF1/COX1 axis on SAH-induced EBI by regulating *miR-19-3*p and GRSF1.

METHODS

Patient and public involvement

No patients were involved.

Experimental animals

Adult male clean Sprague-Dawley (SD) rats (300–350 g) and pregnant rats were purchased from Suzhou Zhaoyan New Drug Research Center (Suzhou, China). All experimental animals were fed under standard conditions.

Establishment of the experimental SAH rat model

Autologous arterial blood was rapidly injected into the anterior cisterna of the optic chiasma to establish a model of SAH in vivo.[27] Details on the experimental design, experimental rat SAH model establishment, primary neuron cultures, lentiviral construction and intervention,[28] mitochondria isolation from brain tissue, reverse transcription PCR (RT-PCR) assay, western blot, immunofluorescence (IF) analysis, terminal deoxynucleotidyl transferase-mediated dUTP nick end labelling (TUNEL) staining, fluoro-Jade C (FJC) staining, transmission electron microscopy (TEM), ATP content detection and behavioural experiments are described in online supplemental materials and methods.

Primary neuron cultures

Primary cortical neurons were derived from embryos of pregnant SD rats (16–18 days).[29] The full details of Hoechst staining, live/dead cell staining, mitochondrial membrane potential (MMP) detection, mitochondrial superoxide indicator measurement and ATP content detection are described in online supplemental materials and methods.

Statistical analysis

Details on statistical analysis are presented in online supplemental materials and methods.

miR-19-3p is upregulated, and mRNA and protein levels of GRSF1 and COX1 are downregulated after SAH

Results are upregulated, and mRNA and protein levels of GRSF1 and COX1 are downregulated after SAH RT-PCR, western blot and IF staining were conducted to detect the changes in *miR-19-3*p, GRSF1 and COX1 expression induced by SAH. First, the *miR-19-3*p levels increased

(p=0.0208, p<0.0001, p=0.0002) and the *GRSF1* mRNA levels decreased (p=0.0106, p<0.0001, p=0.0005) in the 3, 12 and 24 hours post-SAH groups compared with the sham group (figure 1A,B). Moreover, the GRSF1 expression level (p=0.03, p<0.0001, p=0.0143) in the 12, 24 and 48 hours post-SAH groups and the COX1 expression level (p=0.032, p=0.0403, p<0.0001, p=0.0002) in the 6, 12, 24 and 48 hours post-SAH groups were significantly decreased, with the lowest level observed at 24 hours, followed by a gradual recovery for 1 week (figure 1C–E). The IF results showed decreased immunopositivity for both GRSF1 in the 24 hours post-SAH group (p=0.0004) and COX1 in the 6 hours (p=0.0257) and 24 hours (p=0.0086) post-SAH groups compared with the sham group (figure 1F–I). According to these results, *miR-19-3*p, GRSF1 and COX1 were involved in the pathological process of brain injury while GRSF1 and COX1 expression levels were inhibited following SAH. In the first part of the experiment since GRSF1 and COX1 levels reached their lowest level 24 hours after SAH, the ideal time point for the follow-up intervention experiment was determined to be 24 hours following SAH.

Silencing/overexpressing GRSF1 alleviates/aggravates the decrease in GRSF1 and COX1 levels after experimental induction of SAH

Western blot was used to detect the expression of target proteins after Lenti-NC1, Lenti-*GRSF1* shRNA, Lenti-NC2 and Lenti-*GRSF1* treatments (figure 2A–C). Compared with the sham group, the expression levels of GRSF1 (p<0.0001) and COX1 (p=0.0005) were significantly lower in the SAH group. By contrast, the levels of GRSF1 (p=0.0025) and COX1 (p=0.0259) were significantly reduced in the Lenti-*GRSF1* shRNA groups compared with those in the Lenti-NC1 group. The Lenti-*GRSF1* group revealed significantly increased protein levels of GRSF1 (p=0.0001) and COX1 (p=0.0007) compared with the Lenti-NC2 group. Double IF staining of GRSF1 and COX1 showed similar expression trends in neurons after SAH in vivo (figure 2D–G). Specifically, the fluorescence intensities of GRSF1 (p<0.0001) and COX1 (p=0.0003) in the SAH group were weaker than those in the sham group. By contrast, Lenti-*GRSF1* shRNA further weakened the fluorescence intensities of GRSF1 (p=0.0242) and COX1 (p=0.0123) compared with those in the Lenti-NC1 group while Lenti-*GRSF1* increased the weakened fluorescence intensities of GRSF1 (p=0.0003) and COX1 (p=0.0037) compared with those in the Lenti-NC2 group.

Silencing/overexpressing *miR-19-3p* alleviates/aggravates the decreased GRSF1 and COX1 levels in vitro after SAH

The western blot results are shown in figure 3A–C. GRSF1 (p=0.0035) and COX1 (p=0.0023) expression levels were significantly reduced in the oxyhaemoglobin (OxyHb) group. By contrast, the *miR-19-3*p mimic significantly decreased GRSF1 (p=0.0337) and COX1 (p=0.0442) levels while the *miR-19-3*p inhibitor increased the levels of GRSF1 (p=0.0281) and COX1 (p=0.0376) compared with those in the OxyHb group. Analogously, IF staining indicated similar trends, in that OxyHb decreased the fluorescence intensities of GRSF1 (p=0.0012) and COX1 (p=0.0131); the *miR-19-3*p inhibitor significantly increased the fluorescence intensities of GRSF1 (p=0.0255) and COX1 (p=0.0488); and the *miR-19-3*p mimic decreased the fluorescence intensities of GRSF1 (p=0.0127) and COX1 (p=0.0084) in neurons induced by OxyHb (figure 3D–G).

Silencing/overexpressing GRSF1 alleviates/aggravates the decrease in GRSF1 and COX1 levels in vitro after SAH

Western blot was used to assess the expression of target proteins in neurons after treatments with Lenti-NC1, Lenti-*GRSF1* shRNA, Lenti-NC2 and Lenti-*GRSF1* (figure 4A–C). The protein levels of GRSF1 (p=0.0077) and COX1 (p=0.0141) were markedly lower in the OxyHb group compared with those in the Control group. By contrast, the GRSF1 (p=0.0450) and COX1 (p=0.0089) expression levels were significantly lower in the Lenti-*GRSF1* shRNA groups compared with the Lenti-NC1 groups while in comparison with Lenti-NC2 group, Lenti-*GRSF1* significantly increased the GRSF1 (p=0.0348) protein levels. Moreover, IF staining showed that GRSF1-immunopositive cells were decreased (p=0.0454) by Lenti-*GRSF1* shRNA treatment and increased (p=0.0014) by Lenti-*GRSF1* treatment in neurons under OxyHb stimulation (figure 4D,E). Double IF staining revealed that Lenti-*GRSF1* treatment increased (p=0.0010), and Lenti-*GRSF1* shRNA further decreased (p=0.0342) COX1 and ATPB expression in OxyHb-induced neurons (figure 4F,G).

Silencing/overexpressing GRSF1 aggravates/alleviates OxyHb-induced and SAH-induced neuronal damage, apoptosis and degradation

TUNEL staining (figure 5A,B) and FJC staining (figure 5C,D) were used to evaluate the apoptosis and degradation of cortical neurons to determine the effects of the *miR-19-3*p/GRSF1/COX1 axis in SAH-induced EBI. The proportions of TUNEL-positive (p<0.0001) and FJC-positive (p<0.0001) cells were significantly higher in the SAH group than those in the sham group. The proportions of TUNEL-positive (p=0.0029) and FJC-positive (p=0.0314) cells following Lenti-*GRSF1* shRNA treatment were significantly higher compared with those following Lenti-NC1 treatment. In contrast, the proportions of TUNEL-positive (p=0.0035) and FJC-positive (p=0.0033) cells following Lenti-*GRSF1* treatment were significantly lower when compared with those in the Lenti-NC2 group. The effect of GRSF1 on OxyHb-induced neuronal injury was investigated by live/dead cell staining (figure 5E,F). According to the live/dead cell staining results, in the OxyHb group, the ratio of living cells to dead neurons (p=0.0004) was lower than that in the control group. Nevertheless, the neurons

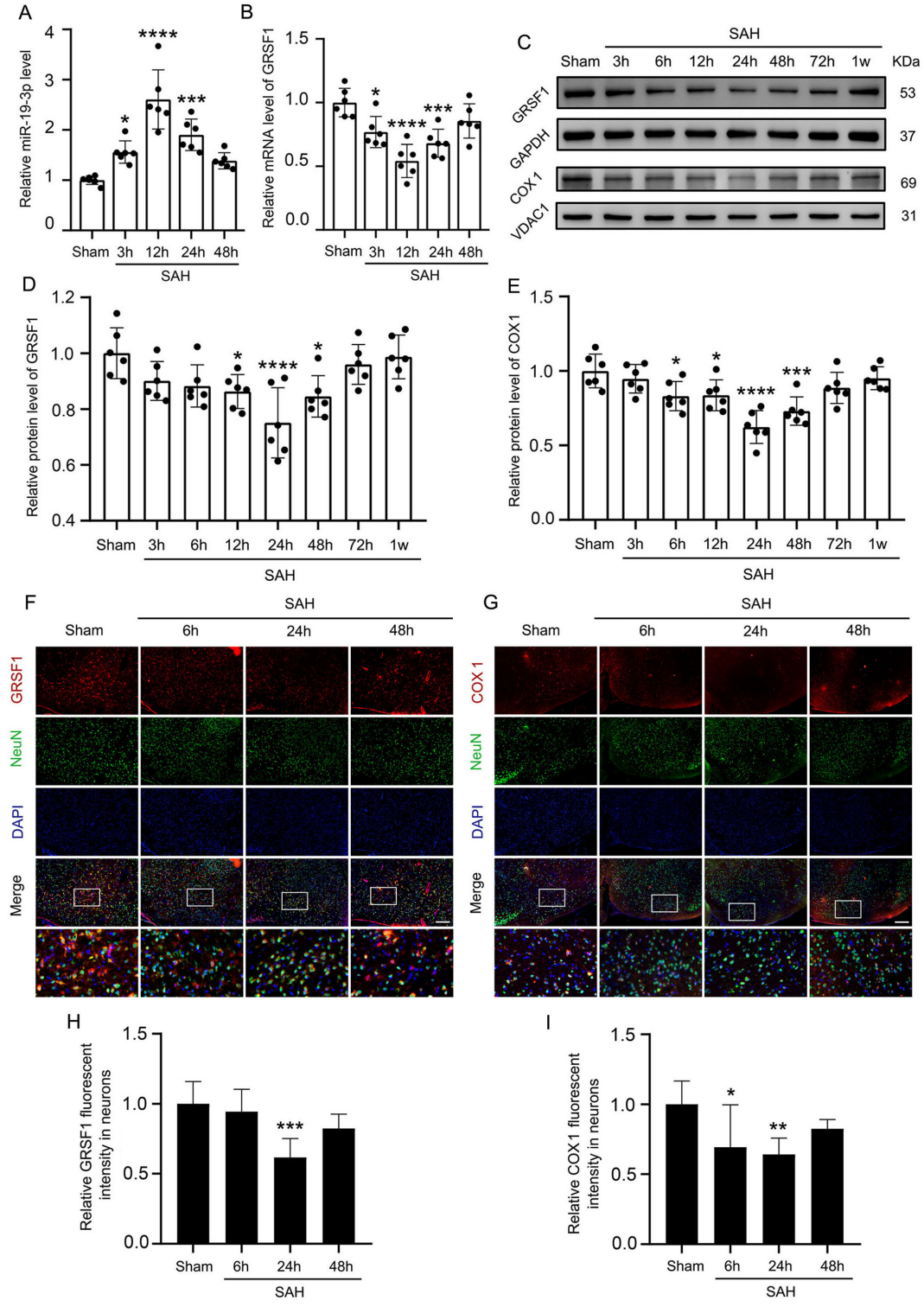

Figure 1 Levels of *miR-19-3*p, GRSF1 mRNA and protein, and COX1 protein, and expression of GRSF1 and COX1 in neurons following SAH. (A, B) Quantitative analysis of *miR-19-3*p and *GRSF1* mRNA levels using the Sham group as a standard. (C) Western blot of GRSF1 and COX1 showed representative bands. (D, E) Quantitative analysis of GRSF1 and COX1 protein levels at different stages after SAH using the Sham group as a standard. (F, G) Double immunofluorescence was performed with GRSF1 and COX1 (red, Alexa Fluor 555) and the neuronal marker (NeuN; green, Alexa Fluor 488). Nuclei were stained with DAPI (blue). GRSF1 and COX1 were mainly located in the neurons. The immunopositivity of GRSF1 and COX1 was significantly decreased at 24 hours after SAH compared with the Sham group. Scale bars: 100 µm. (H, I) Quantitative analysis of GRSF1 and COX1 fluorescence intensity, which was normalised to Sham group. Data are shown as mean±SD (n=6). *p<0.05, **p<0.01, ***p<0.001, ****p<0.0001, vs Sham group (one-way analysis of variance followed by Scheffé's post hoc test). COX1, cytochrome C oxidase 1; DAPI, 4′,6-diamidino-2-phenylindole; GAPDH, glyceraldehyde-3-phosphate dehydrogenase; GRSF1, guanine-rich RNA sequence binding factor 1; SAH, subarachnoid haemorrhage; VDAC1, voltage-dependent anion channel 1.

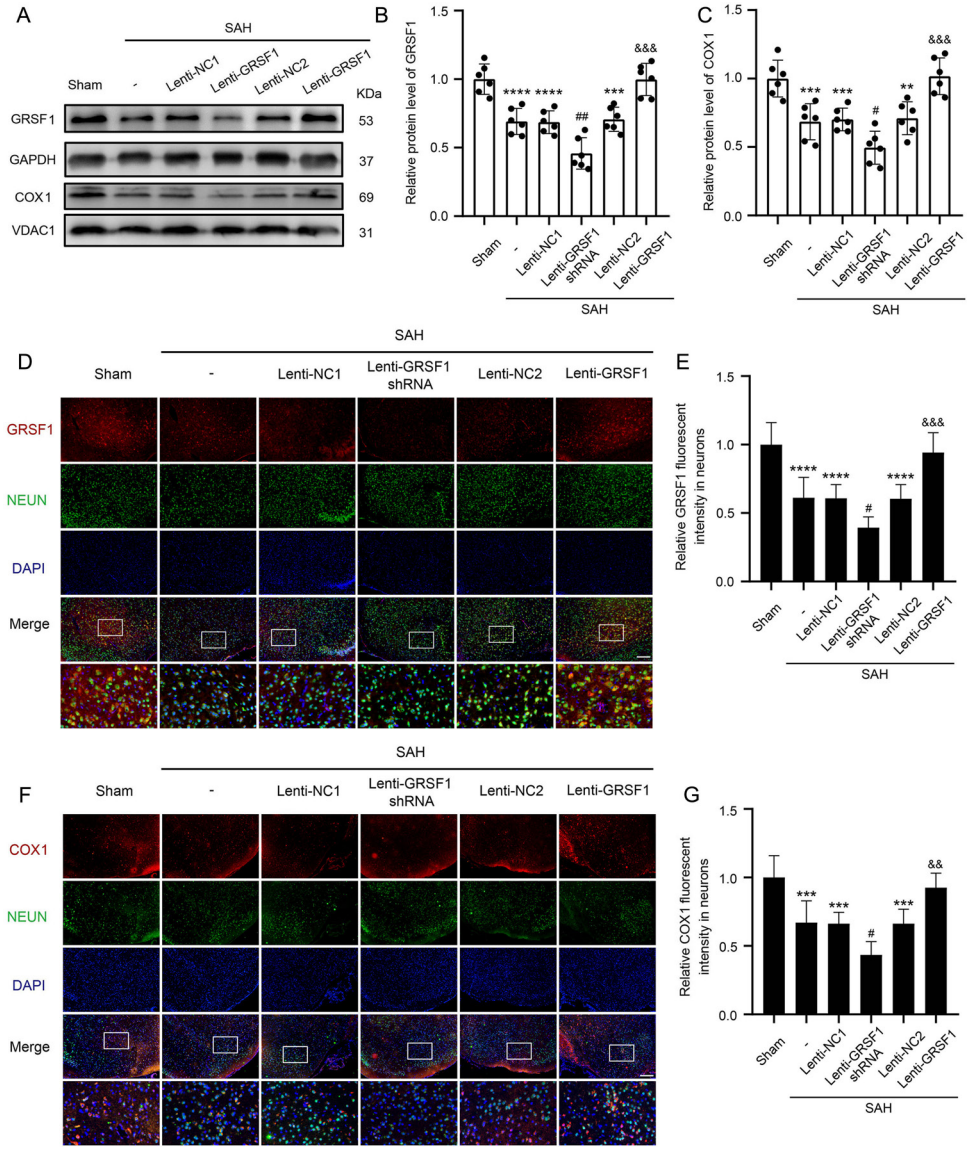

Figure 2 Protein expression levels of GRSF1 and COX1 under Lenti-*GRSF1* shRNA and Lenti-*GRSF1* treatments after in vivo SAH (A) Following in vivo SAH, western blots revealed GRSF1 and COX1 bands under Lenti-*GRSF1* shRNA and Lenti-GRSF1 treatments. (B, C) Quantitative analysis of GRSF1 and COX1 protein levels following in vivo SAH with the Sham group as the standard. (D, F) Double immunofluorescent staining was performed with GRSF1 and COX1 (red, Alexa Fluor 555) and the neuronal marker (NeuN; green, Alexa Fluor 488); nuclei were stained with DAPI (blue). Silencing GRSF1 decreased the neuronal expression of GRSF1 and COX1. Conversely, overexpressing GRSF1 increased the neuronal GRSF1 and COX1 expression. Scale bars: 200 µm. (E, G) Comparative analysis of the expression of GRSF1 and COX1 in different groups using quantitative fluorescent intensity analysis with the Sham group as the standard. Data are shown as the mean±SD (n=6). **p<0.01, ***p<0.001, ****p<0.0001 vs Sham group; #p<0.05, ##p<0.01 vs Lenti-NC1 group; &&p<0.01, &&&p<0.001 vs Lenti-NC2 group (one-way analysis of variance followed by Scheffé's post hoc test). COX1, cytochrome C oxidase 1; DAPI: 4′,6-diamidino-2-phenylindole; GRSF1, guanine-rich RNA sequence binding factor 1; OxyHb, oxyhemoglobin; SAH, subarachnoid haemorrhage; TUNEL, terminal deoxynucleotidyl transferase-mediated dUTP nick end labelling, VDAC1, voltage-dependent anion channel 1.

treated with Lenti-*GRSF1* shRNA had a much lower survival rate (p=0.0056) compared with those in the Lenti-NC1 group. By contrast, the neuronal survival rate (p=0.0455) was higher in the Lenti-*GRSF1* group compared with that in the Lenti-NC2 group. Neuronal apoptosis was roughly assessed by Hoechst staining (figure 5G,H), with the results revealing that OxyHb (p=0.0 003) increased neuron apoptosis, which was further increased by Lenti-*GRSF1* shRNA treatment (p=0.0129) but decreased by Lenti-*GRSF1* (p=0.0451).

Silencing/overexpressing GRSF1 aggravates/alleviates OxyHb-induced mitochondrial fragmentation and MMP in neurons

Mitochondrial fragmentation, in which the mitochondrial network is disrupted and mitochondrial branches are broken, was evaluated by IF staining of

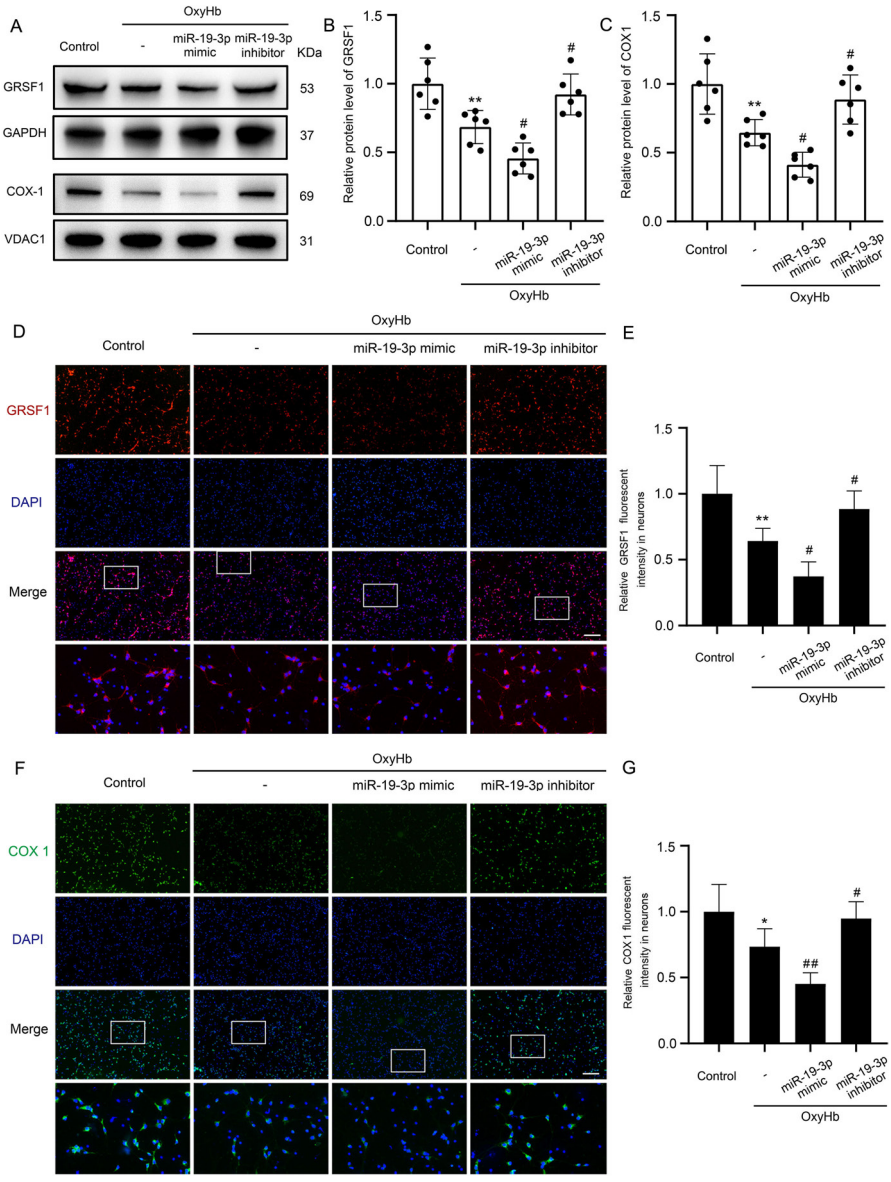

Figure 3 Protein expression levels of GRSF1 and COX1 under *miR-19-3*p mimic and *miR-19-3*p inhibitor treatments after in vitro SAH. (A) Following in vitro SAH, GRSF1 and COX1 bands were detected by western blotting under mimicry or inhibitory treatments with *miR-19-3*p. (B, C) GRSF1 and COX1 quantitative analysis following in vitro SAH in different groups, with the control group as the standard. (D, F) Immunofluorescence of GRSF1 (red, Alexa Fluor 555) and COX1 (green, Alexa Fluor 555) in primary neurons, and nuclei were stained with DAPI (blue). *miR-19-3*p mimic decreased the neuronal GRSF1 and COX1 expression. Conversely, the *miR-19-3*p inhibitor increased the neuronal GRSF1 and COX1 expression. Scale bars: 200 µm. (E, G) Quantitative analysis of GRSF1 and COX1 fluorescent intensity, with the control group as the standard. Data are shown as the mean±SD (n=6). *p<0.05, **p<0.01 vs control group; #p<0.05, ##p<0.01 vs OxyHb group (one-way analysis of variance followed by Scheffé's post hoc test). COX1, cytochrome C oxidase 1; DAPI, 4′,6-diamidino-2-phenylindole; GRSF1, guanine-rich RNA sequence binding factor 1; OxyHb, oxyhaemoglobin; SAH, subarachnoid haemorrhage.

ATPB (figure 6A,B). The result showed that obvious mitochondrial fragmentation was observed in the SAH, Lenti-NC1 and Lenti-NC2 groups (p=0.0008, p=0.0004, p=0.0009) while Lenti-*GRSF1* shRNA aggravated mitochondrial fragmentation in neurons (p=0.0159), and Lenti-*GRSF1* alleviated mitochondrial fragmentation induced by OxyHb for 24 hours (p=0.0321). To investigate the effect of the *miR-19-3*p/GRSF1/COX1 axis on MMP, neurons were stained with JC-1 in vitro. JC-1 fluoresces red when neuronal mitochondria are healthy, but it fluoresces green when damaged (figure 6C,D). The ratio of red to green fluorescence signal in the OxyHb group was lower than that in the Control group (p<0.0001), and Lenti-*GRSF1* shRNA treatment further decreased the ratio of red to green fluorescence signal (p=0.0197) compared with that in the Lenti-NC1 group. In contrast, the ratio of red to green fluorescence signal in the OxyHb+Lenti-*GRSF1* treatment group was

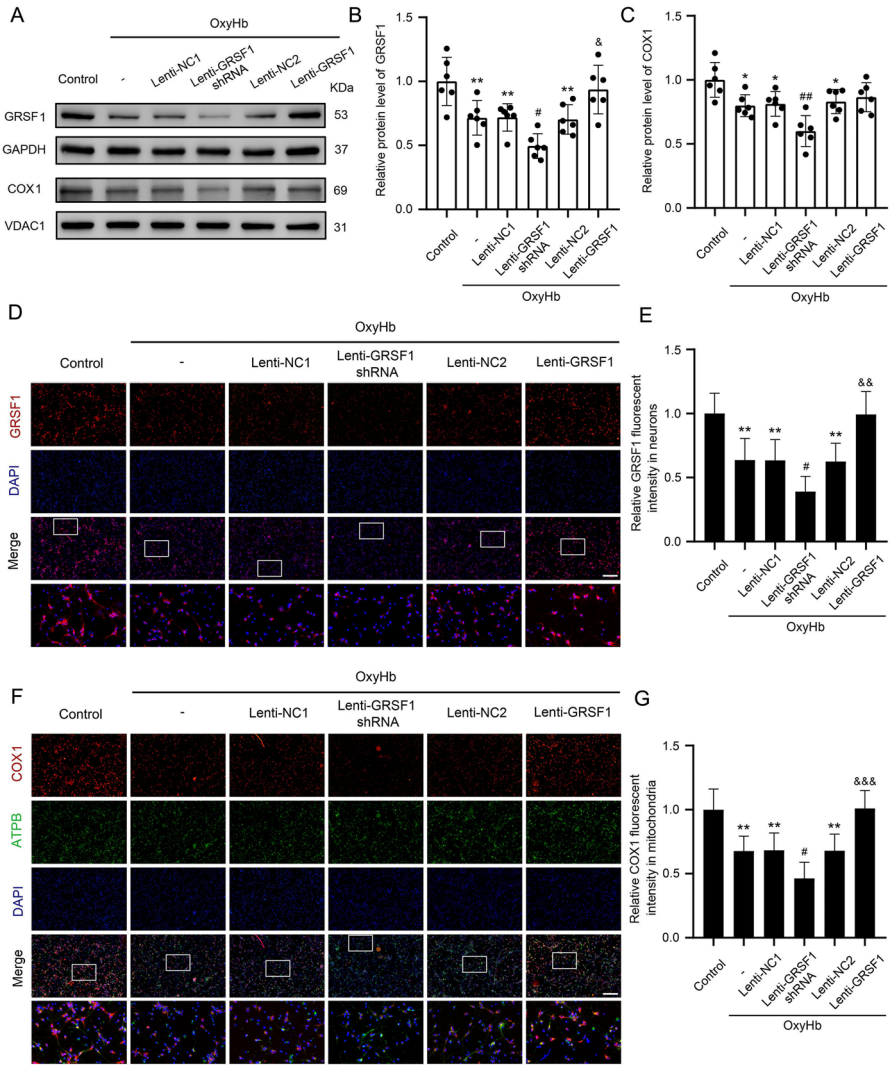

Figure 4 Protein expression levels of GRSF1 and COX1 under Lenti-*GRSF1* shRNA and Lenti-*GRSF1* treatments after in vivo SAH. (A) Following in vitro SAH, western blots showing GRSF1 and COX1 bands were detected under Lenti-*GRSF1* shRNA and Lenti-*GRSF1* treatments. (B, C) Quantitative analysis of GRSF1 and COX1 protein expression levels, with the Control group as the standard. (D) Immunofluorescence of GRSF1 (red, Alexa Fluor 555); nuclei were stained with DAPI (blue). Silencing GRSF1 decreased the neuronal GRSF1 expression. Conversely, overexpressing GRSF1 increased the neuronal GRSF1 expression. (F) Double immunofluorescence analysis of COX1 (red, Alexa Fluor 555) and ATPB (mitochondrial marker, green, Alexa Fluor 488); nuclei were stained with DAPI (blue). Silencing GRSF1 decreased the neuronal COX1 expression. Conversely, overexpressing GRSF1 increased the neuronal COX1 expression. Scale bars: 100 µm. (E, G) Comparative analysis of the expression of GRSF1 and COX1 using quantitative fluorescent intensity analysis. The Control group was regarded as the standard. Data are shown as mean±SD (n=6). *p<0.05, **p<0.01 vs control group; #p<0.05, ##p<0.01 vs Lenti-NC1 group; &p<0.05, &&p<0.01, &&&p<0.001 vs Lenti-NC2 group (one-way analysis of variance followed by Scheffé's post hoc test). ATPB, beta subunit of ATP synthase; COX1, cytochrome C oxidase 1; DAPI, 4′,6-diamidino-2-phenylindole; GRSF1, guanine-rich RNA sequence binding factor 1; SAH, subarachnoid haemorrhage.

higher than that in the OxyHb+Lenti-NC2 group (p=0.0002).

Silencing/overexpressing GRSF1 aggravates/alleviates OxyHb-induced and SAH-induced mitochondrial dysfunction, mitochondrial structure destruction and mitochondrial apoptosis in neurons

We next evaluated the effects of GRSF1 expression on mitochondrial function of OxyHb-treated neurons by detecting the level of mitochondrial superoxide (figure 7A,B), ATP content (figure 7C) and mitochondrial apoptosis (figure 7D,E). When the neurons were treated with OxyHb, the mitochondrial superoxide level was increased (p=0.0005), and the mitochondrial ATP content was obviously reduced (p=0.0002), which was further exacerbated by silencing GRSF1 (p=0.0027, p=0.033) and improved by overexpressing GRSF1 (p=0.0498, p=0.0468). Western blot of cleaved caspase-9 showed that OxyHb significantly increased caspase-9 cleavage in neurons (p=0.002). Silenced GRSF1 further increased (p=0.0019) and overexpressed GRSF1 decreased (p=0.0271), caspase-9

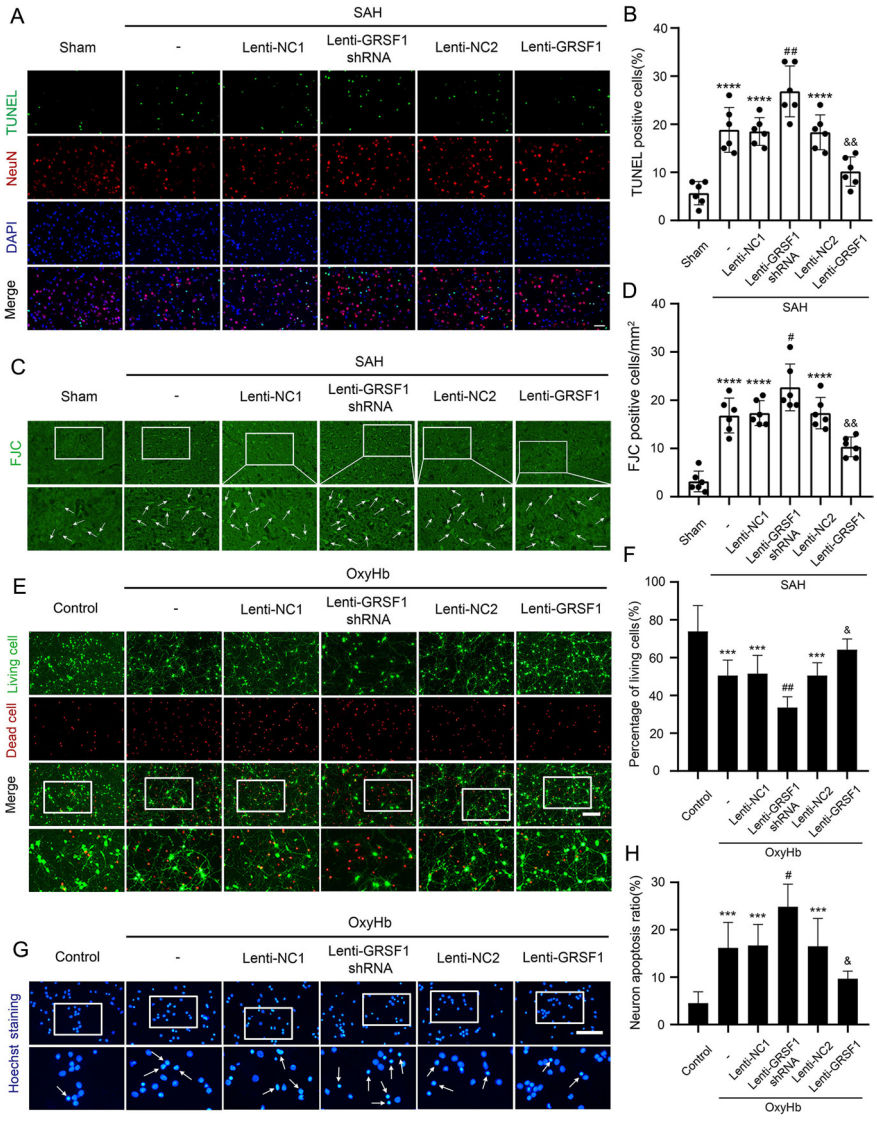

Figure 5 Effect of Lenti-*GRSF1* shRNA and Lenti-*GRSF1* on cortical cell apoptosis and degradation after SAH. (A) TUNEL staining (red, Alexa Fluor 555) and neuronal marker (NeuN, green, Alexa Fluor 488) were used to assess neuronal apoptosis. Silencing GRSF1 suppressed neuronal apoptosis and overexpressing GRSF1 aggravated neuronal apoptosis. Scale bar: 50 µm. (B) Quantitative analysis of the percentage of apoptotic neurons. (C) Neuronal degeneration was evaluated using FJC staining (green), with arrows pointing to cells that were positive for FJC. Silencing GRSF1 suppressed neuronal degeneration and overexpressing GRSF1 aggravated neuronal degeneration. Scale bar: 20 µm. (D) Number of FJC-positive cells/mm^2. (E) Live-dead cellular staining: green staining indicates living neurons and red staining indicates dead neurons. Lenti-*GRSF1* shRNA decreased and Lenti-*GRSF1* improved the survival rates of oxyHb-induced damaged neurons. Scale bar: 100 µm. (F) Quantitative analysis of the percentage of living neurons in different groups. (G) Neuronal apoptosis was evaluated by Hoechst staining. Silencing GRSF1 aggravated neuronal cell apoptosis and overexpressing GRSF1 suppressed neuronal apoptosis. Scale bar: 150 µm. (H) Neuronal apoptosis ratio revealed by Hoechst staining. Data are shown as the mean±SD (n=6). ***p<0.001 vs control group; ****p<0.0001 vs sham group; $^{\#}$p<0.05, $^{\#\#}$p<0.01 vs SAH+Lenti-NC1 group; $^{\#}$p<0.05, $^{\#\#}$p<0.01 vs OxyHb+Lenti-NC1 group; $^{\&\&}$p<0.01 vs SAH+Lenti-NC2 group; $^{\&}$p<0.05 vs OxyHb+Lenti-NC2 group; (one-way analysis of variance followed by Scheffé's post hoc test). COX1, cytochrome C oxidase 1; DAPI, 4′,6-diamidino-2-phenylindole; FJC, Fluoro-Jade C; GRSF1, guanine-rich RNA sequence binding factor 1; OxyHb, oxyhaemoglobin; SAH: subarachnoid haemorrhage; TUNEL, terminal deoxynucleotidyl transferase-mediated dUTP nick end labelling.

cleavage after in vitro SAH, suggesting that GRSF1 upregulation may restrain mitochondria-related apoptosis. We then used TEM to evaluate 4-hydroxynonenal (4-HNE) expression and ATP content to observe the effect of regulating the GRSF1 level on the mitochondrial ultrastructure in neurons and mitochondrial injury surrounding the clot. The representative images of the mitochondrial ultrastructure are shown in figure 7F. We observed that the mitochondrial cristae of neurons were damaged around the clot after SAH (p=0.0002), and the dense mitochondrial cristae structure became loose and chaotic, which was aggravated (p=0.0028) by silencing GRSF1 and alleviated (p=0.0318) by overexpressing GRSF1 (figure 7G). In addition, compared with

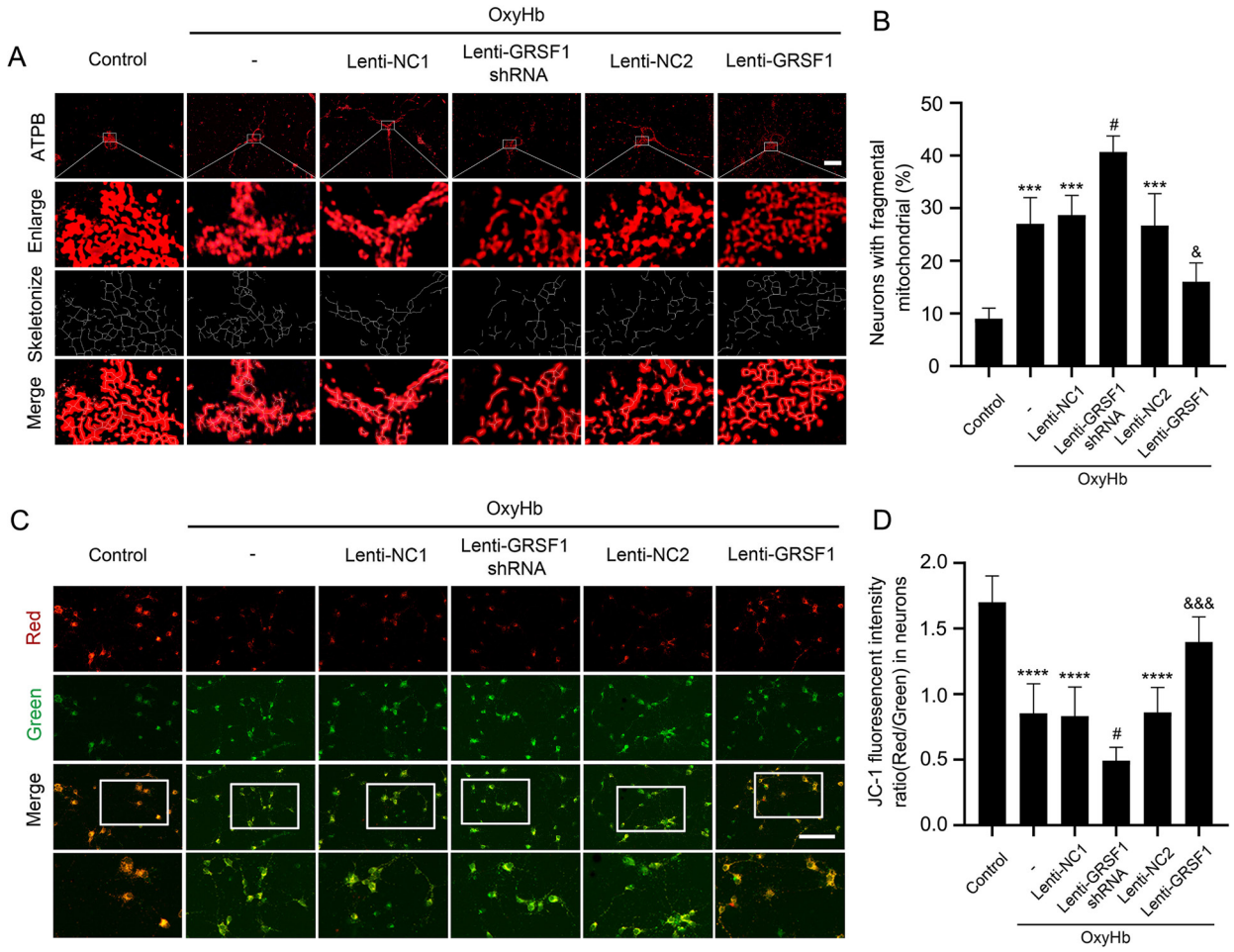

Figure 6 Effect of Lenti-*GRSF1* shRNA and Lenti-*GRSF1* treatments on mitochondrial damage under neuron injury conditions. (A) Immunofluorescence was performed with ATPB antibody (neuronal mitochondrial network, red, Alexa Fluor 555). Silencing GRSF1 aggravated mitochondrial damage while overexpressing GRSF1 relieved mitochondrial damage induced by oxyHb. Scale bars: 20 µm. (B) Quantitative analysis of the percentage of neurons with fragmented mitochondria. Silencing GRSF1 aggravated and overexpressing GRSF1 relieved the percentage of neurons with fragmented mitochondria induced by OxyHb. (C) Changes in mitochondrial membrane potential (ΔΨm). Silencing GRSF1 further reduced mitochondrial membrane potential and overexpressing GRSF1 enhanced OxyHb-induced mitochondrial membrane potential decline in neurons. The presence of red fluorescence represents a normal ΔΨm and a healthy cell state while green fluorescence indicates decreased ΔΨm and cells that are most likely in the early stages of apoptosis. Scale bar: 100 µm. (D) Quantitative analysis of JC-1 fluorescence intensity ratio (red/green) in neurons. Data are shown as the means±SD (n=3). ***p<0.001, ****p<0.0001 vs control group; #p<0.05vs OxyHb+Lenti-NC1 group; &p<0.05, &&&p<0.001 vs OxyHb+Lenti-NC2 group (one-way analysis of variance followed by Scheffé's post hoc test). ATPB, beta subunit of ATP synthase; DAPI, 4′,6-diamidino-2-phenylindole; GRSF1, guanine-rich RNA sequence binding factor 1; OxyHb, oxyhaemoglobin; TUNEL, terminal deoxynucleotidyl transferase-mediated dUTP nick end labelling.

the sham group, the mitochondrial length of neurons was significantly shortened (p<0.0001) after SAH. Silencing of GRSF1 reduced (p=0.0051) the mitochondrial length while the overexpression of GRSF1 increased (p=0.0223) the mitochondrial length in neurons surrounding the clot in SAH rats (figure 7H). Finally, 4-HNE was considered to be an indicator of mitochondrial damage. We found that the 4-HNE level (figure 7J,K) increased (p<0.0001) and the ATP content (p=0.0006) (figure 7I) decreased in the temporal base brain tissue after SAH. Silencing GRSF1 further increased the 4-HNE level (p=0.0003) and decreased the ATP content (p=0.0187) while overexpressing GRSF1 reversed the SAH-induced increase in 4-HNE level (p=0.0027) and decreased the ATP content (p=0.0332).

Silencing GRSF1 aggravates while overexpressing GRSF1 improves SAH-induced neurocognitive function

We next evaluated the behavioural activity of all rats using a behavioural score to determine whether GRSF1 overexpression improves neurological function (figure 8A). A significant deficit in neurological function was observed in the rats following SAH compared with the sham group (p<0.0001), and further aggravation of neurological function impairment was observed in the Lenti-*GRSF1* shRNA group (p=0.0469). The neurological deficits were significantly improved in the Lenti-*GRSF1*

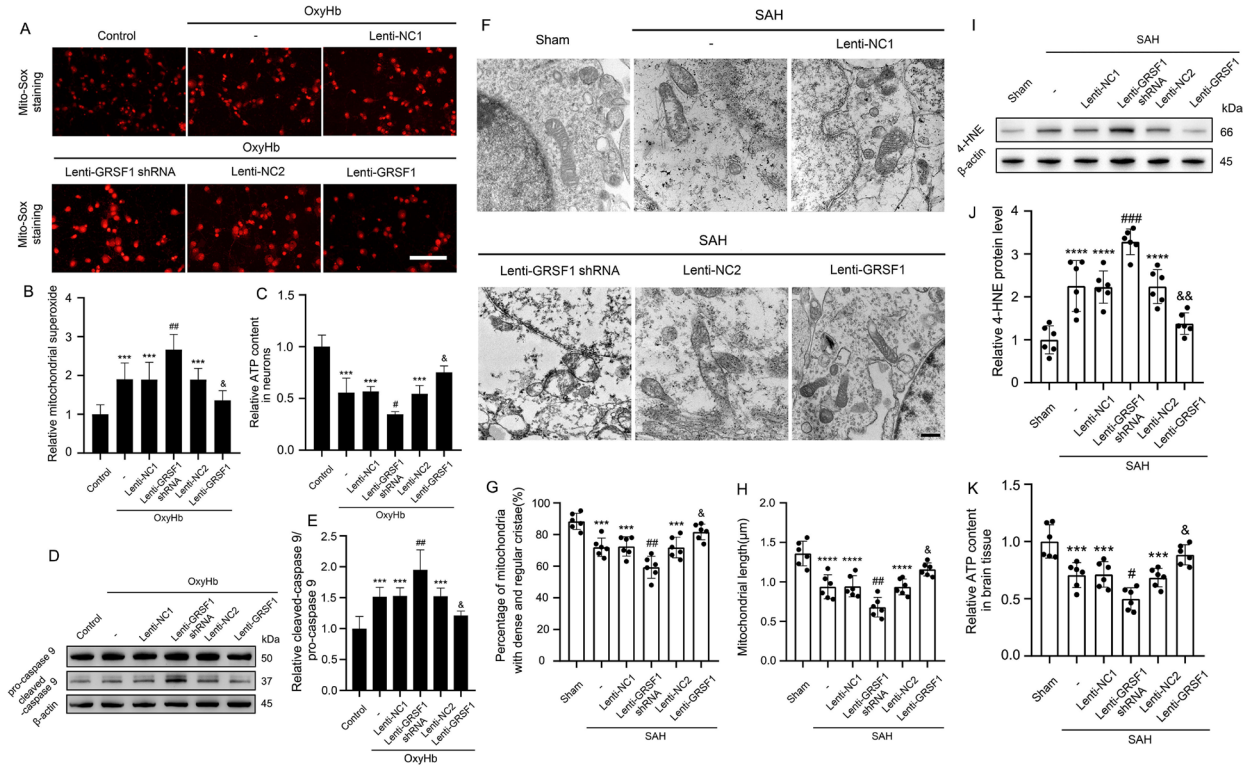

Figure 7 Effect of Lenti-*GRSF1* shRNA and Lenti-*GRSF1* treatments on mitochondrial superoxide generation, mitochondrial bioenergetic deficits and mitochondrial apoptosis after in vitro SAH. (A) Representative fluorescent images of Mito-Sox staining (red) among different groups in in vitro SAH after 24 hours. Scale bars: 100 µm. (B) Quantitative analysis of mitochondrial superoxide in neurons. Silencing GRSF1 further enhanced and overexpressing GRSF1 reduced, OxyHb-induced superoxide generation in neurons. (C) Quantitative analysis of the ATP content in neurons. Silencing GRSF1 enhanced and overexpressing GRSF1 reduced, the ATP content in neurons after in vitro SAH. (D) Western blots showing representative caspase-9 and cleaved caspase-9 bands that were detected under Lenti-*GRSF1* shRNA and Lenti-*GRSF1* treatments. (E) Quantitative analysis of the ratio of cleaved caspase-9 to caspase-9 in neurons. Silencing GRSF1 enhanced and overexpressing GRSF1 reduced, OxyHb-induced mitochondrial apoptosis in neurons. Data are shown as the means±SD (n=6). (F) Representative transmission electron microscopy images of neuronal mitochondria. Mitochondria in the control group had dense cristae and an appropriate mitochondrial length, but mitochondrial oedema appeared, and the length was shortened following the addition of OxyHb. Silencing GRSF1 impaired mitochondrial cristae oedema while overexpressing GRSF1 alleviated it. Scale bar: 0.5 µm. (G) Quantitative analysis for the proportion of mitochondria with fine and dense cristae. (H) Quantitative analysis for the mitochondrial length from each group. (I) Western blot showing representative 4-HNE bands detected under Lenti-*GRSF1* shRNA and Lenti-*GRSF1* treatments. (J) Quantitative analysis of the 4-HNE protein expression level, with the sham group as the standard. (K) Quantitative analysis of the ATP content in brain tissue. Data are shown as the means±SD (n=6). ***p<0.001, ****p<0.0001 vs control group or sham group; #p<0.05, ##p<0.01, ###p<0.001 vs OxyHb+Lenti-NC1 group or SAH+Lenti-NC1 group; &p<0.05, &&p<0.01 vs OxyHb+Lenti-NC2 group or SAH+Lenti-NC2 group (one-way analysis of variance followed by Scheffé's post hoc test). GRSF1, guanine-rich RNA sequence binding factor 1; 4-HNE, 4-hydroxynonenal; OxyHb, oxyhaemoglobin; SAH, subarachnoid haemorrhage.

treatment group (p=0.0469). The locomotor function of rats was also assessed by using the rotarod test at 3, 7, 14, 21 and 28 days after SAH (figure 8B). The motor ability of rats was severely impaired after SAH (p<0.0001) and was further exacerbated by silencing GRSF1 (p=0.0168) while the recovery was accelerated by overexpression of GRSF1 (p=0.0318). We also performed an adhesive removal test to assess the coordination and sensorimotor function of rats at 3, 7, 14, 21 and 28 days after SAH (figure 8C). After SAH, the rats took longer to remove the stickers (p<0.0001), with significantly longer durations observed when GRSF1 was decreased (p=0.0069). However, when GRSF1 was increased, the duration was markedly shortened (p=0.0178). Finally, the Morris water maze experiment was applied to study the spatial and motor learning abilities of rats after SAH. The representative trajectories of the rats in different groups are shown in figure 8D–I. A significant increase in escape latency (figure 8J) was recorded in the SAH group in the Morris water maze test (p<0.0001). Moreover, the Lenti-*GRSF1* shRNA group had a longer escape latency after SAH than the Lenti-NC1 group (p=0.0003) while the escape latency in the Lenti-*GRSF1* group was shorter than that in the Lenti-NC2 group (p=0.0034). The swimming distance (figure 8K) was significantly increased in the SAH group, Lenti-NC1 group and Lenti-NC2 group (all p<0.0001). According to the results, the swimming distance of the Lenti-*GRSF1* shRNA group was obviously longer than that

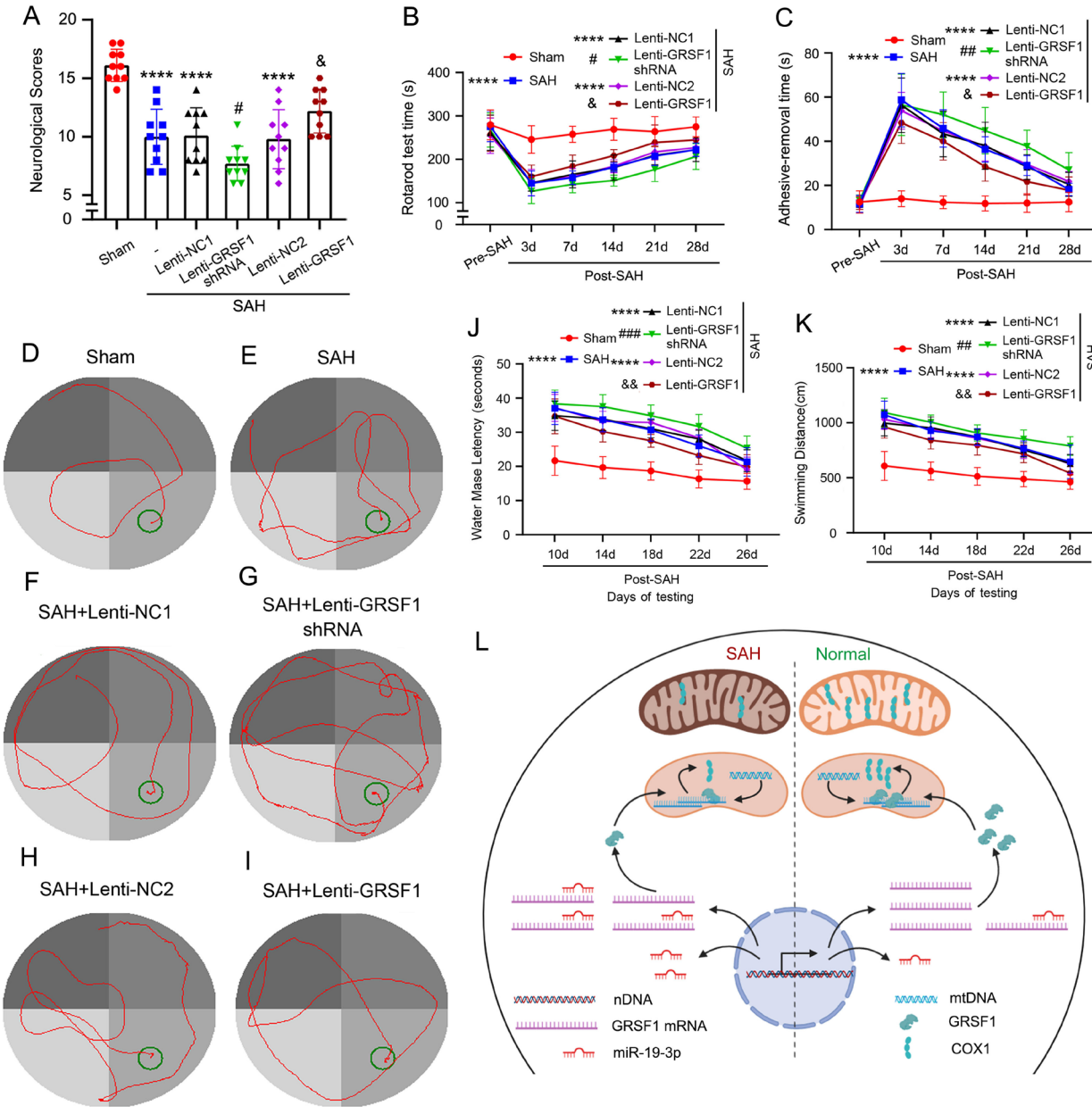

Figure 8 Effect of silenced/overexpressed GRSF1 on neurological scores, sensory and locomotor function recovery, and spatial and motor learning ability of rats after SAH (A) Neurological scoring. (B) Rotarod test. When GRSF1 was silenced, rats lost locomotor function after SAH. When GRSF1 was overexpressed, rats recovered locomotor function more quickly. (C) Adhesive removal test. Overexpressing GRSF1 after SAH accelerated sensory recovery while silencing GRSF1 delayed it. (D–I) The red line represents the rats' swimming tracks. Silencing and overexpressing GRSF1 resulted in longer and shorter swimming trajectories, respectively. The green circle indicates where the target platform is placed. (J) Escape latency in the Morris water maze. Silencing and overexpressing GRSF1 increased and decreased the escape latency, respectively. (K) Swimming distance in the Morris water maze. Silencing and overexpressing GRSF1 increased and decreased the swimming distance, respectively. (L) Roles of the *miR-19-3* p/GRSF1/COX1 axis in SAH-induced EBI. GRSF1 and COX1 are involved in maintaining the integrity of the mitochondrial respiratory chain under normal circumstances. GRSF1/COX1 protein levels were significantly reduced following SAH while *miR-19-3*p levels were increased. Furthermore, inhibition of the *miR-19-3*p/GRSF1/COX1 axis aggravated SAH-induced EBI. Hence, the *miR-19-3*p/GRSF1/COX1 axis may play a neuroprotective role after SAH by maintaining normal mitochondrial function. Data are shown as the mean±SD (n=8). ****p<0.0001 vs sham group; $^{\#}$p<0.05, $^{\#\#}$p<0.01, $^{\#\#\#}$p<0.001 vs Lenti-NC1 group; $^{\&}$p<0.05, $^{\&\&}$p<0.01 vs Lenti-NC2 group (two-way analysis of variance followed by Scheffé's post hoc test). COX1, Cytochrome C oxidase 1; EBI, early brain injury; GRSF1, guanine-rich RNA sequence binding factor 1; mtDNA, mitochondrial DNA; nDNA, nuclear DNA; SAH, subarachnoid haemorrhage.

of the Lenti-NC1 group (p=0.0012) while compared with the Lenti-NC2 group, the swimming distance of the Lenti-*GRSF1* group was significantly shorter (p=0.0085).

DISCUSSION

In this study, primary neurons were extracted, cultured and treated with OxyHb to analyse the key factors leading

to the abnormal mitochondrial function of neurons after SAH. We observed that GRSF1 and COX1 were downregulated by previous proteomic analysis, western blot and IF. Hence, this experiment revealed that the *miR-19-3*p/GRSF1/COX1 axis could be regarded as a novel research target. Our results suggested that the *miR-19-3*p level significantly increased, and the *GRSF1* mRNA level decreased after SAH, which was accompanied by the decreased protein levels of GRSF1 and COX1 in SAH-induced brain tissue. In addition, the *miR-19-3*p inhibitor increased the protein levels of GRSF1 and COX1 in cultured neurons while *miR-19-3*p mimic decreased these levels. Besides, Lenti-*GRSF1* shRNA decreased, and Lenti-*GRSF1* increased, the protein levels of GRSF1 and COX-1 in the brain tissue and neurons. Lenti-*GRSF1* shRNA also aggravated indicators of brain injury, including apoptosis, degeneration and death of cortical and primary neurons, and cognitive impairment in both in vitro and in vivo SAH conditions. In contrast, Lenti-*GRSF1* attenuated these effects by reducing mitochondrial damage and maintaining mitochondrial integrity inside neurons. More importantly, the *miR-19-3*p/GRSF1/COX1 axis may be a potential target to inhibit SAH-induced EBI by maintaining mitochondrial integrity. The results of this experiment systematically elaborate that the activation of the *miR-19-3*p/GRSF1/COX1 axis positively facilitates brain injury repair and neurological function recovery.

Four mitochondrial targeting prediction programmes have predicted that GRSF1 localises to mitochondria. GRSF1, an RNA-binding protein, was first reported to interact specifically with 50 UTRs of viral cytosolic mRNAs, mainly targeting mitochondria and localising to RNA particles close to the mitochondrial nucleolus.[23 30] GRSF1 exists in the nucleus, cytoplasm and mitochondria and is involved in a variety of physiological processes and in the pathogenesis of various diseases. Thus, as mitochondrial RNAs are translated, processed and stored, GRSF1 appears to be necessary to coordinate several aspects of this process.[22] When GRSF1 is lost or decreased, mRNAs and rRNAs are destabilised, RNA loading on ribosomes is dysregulated, ribosomal biogenesis is abnormal and mitochondrial protein synthesis is dysregulated.[31] Previous research has shown that the knockdown of GRSF1 expression brought about a combined oxidative phosphorylation (OXPHOS) and COX assembly defect, which caused abnormalities in the mitochondrial respiratory chain, the extent of which depends on the residual level of GRSF1. Specifically, GRSF1 acts as an RNA-binding protein to promote the translation of COX1 mRNA, and the COX1 level is regulated by GRSF1 expression.[32] Previous research on GRSF1 has mainly focused on metabolic diseases and diseases related to mitochondrial abnormalities and malignant tumours,[33 34] which have been less studied in acute stroke. It has been shown that GRSF1-mediated MiRNA-G-1 causes cervical cancer cells to exhibit malignant behaviour and nuclear autophagy by directly upregulating transmembrane p24 trafficking protein 5 and lamin B1.[35] Moreover, GRSF1 promotes tumour growth and epithelial-mesenchymal transition-mediated metastasis in gastric cancer through the Phosphatidylinositol-3-kinase/Protein kinase B pathway.[36] In a previous study of spinal cord injury, a valuable conclusion is presented that GRSF1 attenuates neuronal ferroptosis and promotes functional recovery via GPX4.[24] This experiment showed that GRSF1 expression is associated with SAH-induced brain injury, where it directly affects the synthesis of COX1 and the integrity of the respiratory chain. In the context of SAH, the *miR-19-3*p/GRSF1/COX1 axis underwent a significant suppression, and GRSF1 played a crucial bridging role within the *miR-19-3*p/GRSF1/COX1 axis. Although GRSF1 itself, acting as an RNA-binding protein, does not participate in the synthesis of respiratory chains, it influences and regulates the normal synthesis of mitochondrial respiratory chain proteins by specifically binding to COX1 mRNA. Therefore, upregulation of GRSF1 can significantly alleviate mitochondrial neuronal damage induced by SAH and improve neural function injury.

It is well known that the integrity of the mitochondrial respiratory chain structure is the basis for maintaining normal mitochondrial function. Cells consume oxygen primarily through mitochondrial COX, which produces aerobic energy through ATP.[16] As a highly hydrophobic protein spanning 12 transmembrane domains, COX1 plays a significant role in cellular respiration. Complex IV or COX is the terminal enzyme in the electron transport chain. Mammalian COX is composed of 14 subunits that catalyse cytochrome c oxidation and the reduction of molecular oxygen (O_2) to water (H_2O).[37 38] By releasing energy from redox reactions, the enzyme pumps protons into the intermembrane space from the mitochondrial matrix.[39] Mitochondrial COX deficiency is a mitochondrial disease in the OXPHOS subclass of diseases characterised by defects in COX biogenesis and/or function in the OXPHOS subclass of diseases.[40] It is important to note that there are several distinct types of COX deficiency with different genetic, pathophysiological and clinical characteristics despite their common molecular and biochemical characteristics.[41] Although COX1 is an important component of the mitochondrial respiratory chain, it has not been previously shown to be involved in acute stroke, including haemorrhagic stroke and ischaemic stroke. In this study, we discovered that the level of COX1 significantly decreased after in vitro and in vivo SAH. Currently, there are limited ways to enhance COX1 levels when COX1 synthesis is inhibited. However, it seems feasible to increase the COX1 level by enhancing the levels of the upstream *miR-19-3*p and GRSF1, especially in in vivo SAH. This scheme was conducted and verified in both primary neurons and experimental rats. Finally, it is worth noting that the indirectly upregulated COX1 level caused by increasing GRSF1 inhibited mitochondrial and neuronal damage and improved neurological impairment of experimental rats. Therefore, maintaining normal levels of COX1 might improve the prognosis of patients with SAH.

Given the above-mentioned research results, we came to the following conclusions: Under normal circumstances, the level of GRSF1 in neurons remains moderate and the protein is found in the mitochondria, where it promotes COX1 mRNA translation; COX1 participates in the assembly of the mitochondrial respiratory chain complex and maintains normal mitochondrial function; in contrast, under SAH circumstances, some haematoma component or pathological stimulation leads to a significant increase in *miR-19-3*p, which inhibits *GRSF1* mRNA translation, resulting in a decrease in GRSF1 and even a lack of GRSF1 in mitochondria, especially in the distal mitochondria of neuronal axons; thus, the COX1 mRNA translation device and respiratory chain become incomplete, and eventually, damaged mitochondria cause neuronal and brain damage (figure 8I).

Although we have conducted experiments in both cells and animals, this study still has some limitations. The upstream mechanism of GRSF1/COX1 has not been extensively explored, and an upstream intervention experiment could be performed to further validate our results. In conclusion, the obvious decline in the level of GRSF1 leads to disordered assembly of the respiratory chain, and the decline in GRSF1 mediated by *miR-19-3*p may be an important cause of impaired mitochondrial function. After SAH, controlling the level of GRSF1 in neurons within an appropriate range may be beneficial to protecting neuronal mitochondria and improving neuronal injury. We hope to have clarified the role of the *miR-19-3*p/GRSF1/COX1 axis and its mechanism in the context of brain injury after SAH and provided new ideas and insights for treating patients with SAH.

Contributors Experiment implementation and paper writing: GG; Design of original data analysis strategy: XY S; Preparation of experimental materials, methods, and literature review: JJ X; Manuscript correcting and reviewing: J Y. Experimental design, quality assurance, and control: YW. JY and YW were responsible for the overall content as guarantors. All authors read and agreed to the final manuscript. GG, XY S and JJ X contributed equally to this paper.

Funding This study was funded by National Natural Science Foundation of China (82301471), Fundamental Research Funds for the Central Universities (WK9110000112, WK9110000199) and Anhui Provincial Natural Science Foundation of China (1708085QH174, 2108085MH273).

Competing interests None declared.

Patient consent for publication Not applicable.

Ethics approval All experiments were approved and supervised by the Ethics Committee of the First Affiliated Hospital of University of Science and Technology of China (approval No. 2021-NC(A)-132).

Provenance and peer review Not commissioned; externally peer reviewed.

Data availability statement Data are available on reasonable request.

Author note Experiment implementation and paper writing: GG; Design of original data analysis strategy: XY S; Preparation of experimental materials, methods, and literature review: JJ X; Manuscript correcting and reviewing: J Y. Experimental design, quality assurance, and control: YW. JY and YW were responsible for the overall content as guarantors. All authors read and agreed to the final manuscript. GG, XY S and JJ X contributed equally to this paper.

ORCID iD

Yang Wang http://orcid.org/0000-0002-3870-7293

REFERENCES

1 Neifert SN, Chapman EK, Martini ML, *et al*. Aneurysmal Subarachnoid Hemorrhage: the Last Decade. *Transl Stroke Res* 2021;12:428–46.
2 Maher M, Schweizer TA, Macdonald RL. Treatment of Spontaneous Subarachnoid Hemorrhage: Guidelines and Gaps. *Stroke* 2020;51:1326–32.
3 Lin F, Li R, Tu W-J, *et al*. An Update on Antioxidative Stress Therapy Research for Early Brain Injury After Subarachnoid Hemorrhage. *Front Aging Neurosci* 2021;13:772036.
4 Demura M, Ishii H, Takarada-Iemata M, *et al*. Sympathetic Nervous Hyperactivity Impairs Microcirculation Leading to Early Brain Injury After Subarachnoid Hemorrhage. *Stroke* 2023;54:1645–55.
5 Rass V, Helbok R. Early Brain Injury After Poor-Grade Subarachnoid Hemorrhage. *Curr Neurol Neurosci Rep* 2019;19:78.
6 Zhang Z, Zhang A, Liu Y, *et al*. New Mechanisms and Targets of Subarachnoid Hemorrhage: A Focus on Mitochondria. *Curr Neuropharmacol* 2022;20:1278–96.
7 Yogev S, Shen K. Establishing Neuronal Polarity with Environmental and Intrinsic Mechanisms. *Neuron* 2017;96:638–50.
8 Funahashi Y, Watanabe T, Kaibuchi K. Advances in defining signaling networks for the establishment of neuronal polarity. *Curr Opin Cell Biol* 2020;63:76–87.
9 Goaillard J-M, Moubarak E, Tapia M, *et al*. Diversity of Axonal and Dendritic Contributions to Neuronal Output. *Front Cell Neurosci* 2019;13:570.
10 Han SM, Baig HS, Hammarlund M. Mitochondria Localize to Injured Axons to Support Regeneration. *Neuron* 2016;92:1308–23.
11 Zheng Y, Zhang X, Wu X, *et al*. Somatic autophagy of axonal mitochondria in ischemic neurons. *J Cell Biol* 2019;218:1891–907.
12 Xiao Z-P, Lv T, Hou P-P, *et al*. Sirtuin 5-Mediated Lysine Desuccinylation Protects Mitochondrial Metabolism Following Subarachnoid Hemorrhage in Mice. *Stroke* 2021;52:4043–53.
13 García-Bartolomé A, Peñas A, Marín-Buera L, *et al*. Respiratory chain enzyme deficiency induces mitochondrial location of actin-binding gelsolin to modulate the oligomerization of VDAC complexes and cell survival. *Hum Mol Genet* 2017;26:2493–506.
14 Gopal RK, Calvo SE, Shih AR, *et al*. Early loss of mitochondrial complex I and rewiring of glutathione metabolism in renal oncocytoma. *Proc Natl Acad Sci U S A* 2018;115:E6283–90.
15 Zalewska A, Szarmach I, Żendzian-Piotrowska M, *et al*. The Effect of N-Acetylcysteine on Respiratory Enzymes, ADP/ATP Ratio, Glutathione Metabolism, and Nitrosative Stress in the Salivary Gland Mitochondria of Insulin Resistant Rats. *Nutrients* 2020;12:458.
16 Timón-Gómez A, Nývltová E, Abriata LA, *et al*. Mitochondrial cytochrome c oxidase biogenesis: Recent developments. *Semin Cell Dev Biol* 2018;76:163–78.
17 Mays J-N, Camacho-Villasana Y, Garcia-Villegas R, *et al*. The mitoribosome-specific protein mS38 is preferentially required for synthesis of cytochrome c oxidase subunits. *Nucleic Acids Res* 2019;47:5746–60.
18 Dahal S, Siddiqua H, Katapadi VK, *et al*. Characterization of G4 DNA formation in mitochondrial DNA and their potential role in mitochondrial genome instability. *FEBS J* 2022;289:163–82.
19 Basu U, Bostwick AM, Das K, *et al*. Structure, mechanism, and regulation of mitochondrial DNA transcription initiation. *J Biol Chem* 2020;295:18406–25.
20 Boehm E, Zaganelli S, Maundrell K, *et al*. FASTKD1 and FASTKD4 have opposite effects on expression of specific mitochondrial RNAs, depending upon their endonuclease-like RAP domain. *Nucleic Acids Res* 2017;45:6135–46.
21 Antonicka H, Shoubridge EA. Mitochondrial RNA Granules Are Centers for Posttranscriptional RNA Processing and Ribosome Biogenesis. *Cell Rep* 2015;10:920–32.

22 Jourdain AA, Koppen M, Wydro M, *et al*. GRSF1 regulates RNA processing in mitochondrial RNA granules. *Cell Metab* 2013;17:399–410.
23 Dumoulin B, Ufer C, Kuhn H, *et al*. Expression Regulation, Protein Chemistry and Functional Biology of the Guanine-Rich Sequence Binding Factor 1 (GRSF1). *J Mol Biol* 2021;433:166922.
24 Wang J, Lu J, Zhu Y, *et al*. Guanine-rich RNA sequence binding factor 1 regulates neuronal ferroptosis after spinal cord injury in rats via the GPX4 signaling pathway. *Brain Res* 2023;1818:148497.
25 Grinchuk OV, Jenjaroenpun P, Orlov YL, *et al*. Integrative analysis of the human cis-antisense gene pairs, miRNAs and their transcription regulation patterns. *Nucleic Acids Res* 2010;38:534–47.
26 Hamblin MH, Murad R, Yin J, *et al*. Modulation of gene expression on a transcriptome-wide level following human neural stem cell transplantation in aged mouse stroke brains. *Exp Neurol* 2022;347:113913.
27 Wang Y, Gao A, Xu X, *et al*. The Neuroprotection of Lysosomotropic Agents in Experimental Subarachnoid Hemorrhage Probably Involving the Apoptosis Pathway Triggering by Cathepsins via Chelating Intralysosomal Iron. *Mol Neurobiol* 2015;52:64–77.
28 Cao C, Ding J, Cao D, *et al*. TREM2 modulates neuroinflammation with elevated IRAK3 expression and plays a neuroprotective role after experimental SAH in rats. *Neurobiol Dis* 2022;171:105809.
29 Li X, Li H, Xu Z, *et al*. Ischemia-induced cleavage of OPA1 at S1 site aggravates mitochondrial fragmentation and reperfusion injury in neurons. *Cell Death Dis* 2022;13:321.
30 Hensen F, Potter A, van Esveld SL, *et al*. Mitochondrial RNA granules are critically dependent on mtDNA replication factors Twinkle and mtSSB. *Nucleic Acids Res* 2019;47:3680–98.
31 Liu D, Xu C, Gong Z, *et al*. GRSF1 antagonizes age-associated hypercoagulability via modulation of fibrinogen mRNA stability. *Cell Death Dis* 2023;14:717.
32 Antonicka H, Sasarman F, Nishimura T, *et al*. The mitochondrial RNA-binding protein GRSF1 localizes to RNA granules and is required for posttranscriptional mitochondrial gene expression. *Cell Metab* 2013;17:386–98.
33 Brownmiller T, Caplen NJ. The HNRNPF/H RNA binding proteins and disease. *Wiley Interdiscip Rev RNA* 2023;14:e1788.
34 Sun Q, Yang Z, Li P, *et al*. A novel miRNA identified in GRSF1 complex drives the metastasis via the PIK3R3/AKT/NF-κB and TIMP3/MMP9 pathways in cervical cancer cells. *Cell Death Dis* 2019;10:636.
35 Yang Z, Sun Q, Guo J, *et al*. GRSF1-mediated MIR-G-1 promotes malignant behavior and nuclear autophagy by directly upregulating TMED5 and LMNB1 in cervical cancer cells. *Autophagy* 2019;15:668–85.
36 Wang B, Wang L, Lu Y, *et al*. GRSF1 promotes tumorigenesis and EMT-mediated metastasis through PI3K/AKT pathway in gastric cancer. *Biochem Biophys Res Commun* 2021;555:61–6.
37 Spinazzi M, Casarin A, Pertegato V, *et al*. Assessment of mitochondrial respiratory chain enzymatic activities on tissues and cultured cells. *Nat Protoc* 2012;7:1235–46.
38 Brischigliaro M, Zeviani M. Cytochrome c oxidase deficiency. *Biochim Biophys Acta Bioenerg* 2021;1862:148335.
39 Kadenbach B. Complex IV - The regulatory center of mitochondrial oxidative phosphorylation. *Mitochondrion* 2021;58:296–302.
40 Garone C. Mitochondrial Cytochrome C deficiency can show the first disease signs in the prenatal stage. *Eur J Hum Genet* 2023;31:1344–5.
41 Rak M, Bénit P, Chrétien D, *et al*. Mitochondrial cytochrome c oxidase deficiency. *Clin Sci (Lond)* 2016;130:393–407.